Analysis of Bilateral Coplanar Waveguides Printed on Anisotropic Substrates for Use in Monolithic MICs

Yinchao Chen and Benjamin Beker, *Member, IEEE*

Abstract—**The spectral-domain method is applied to the analysis of bilateral (double-sided) coplanar waveguides that are printed on electric and/or magnetic anisotropic substrates. A non-decoupling approach is used to solve the coupled differential equations for the transverse propagation constants inside the substrate. The dyadic admittance Green's function is derived for both open and shielded bilateral coplanar waveguides, taking into account the anisotropy of the material. Finally, numerical results, describing the propagation characteristics of these structures, are presented for both electric and magnetic wall symmetries.**

I. Introduction

THE IMPORTANCE of the coplanar waveguide, especially in monolithic MICs, stems from the ease of integration of this structure in three terminal devices such as the field effect transistors [1]. This structure also naturally provides the grounding point that can be located close to the device. Additional conductor backing, [2], serves as a convenient on-circuit heat sink [3], though it also provides the means for leakage loss to the parallel plate mode propagating away from the central conductor [1], [12].

The use of coplanar waveguides (CPWs) was first proposed by Wen in 1969 [4]. Whereas the initial work was based on the quasi-static approximation, subsequent efforts involved the full-wave analysis [5]. In addition to research on the coplanar structures printed on isotropic substrates, effects of substrate anisotropy were recently studied as well. In particular, the influence of dielectric anisotropy on the dispersion characteristics of open CPWs was investigated by both the quasi-static and hybrid mode approach [6]. Coplanar waveguides on magnetically anisotropic substrates were analyzed as well, with a detailed treatment available in [7]. Transmission lines based on the asymmetric CPW with finite metallization thickness that are printed on either dielectric or magnetic substrate were also examined, with numerous results reported for frequencies up to 30 GHz [8].

In this paper, effects of substrate anisotropy on the dispersion properties of open and shielded bilateral coplanar waveguides (BCPWs), that are shown in Figs. 1 and 2, are examined. As opposed to the earlier work, the substrate material under consideration herein exhibits both dielectric and magnetic anisotropy at the same time. The spectral-domain method, [9, ch. 5], is employed to derive the dyadic admittance Green's functions of two BCPW structures. Maxwell's equations are reduced to a set of two coupled differential equations of second order for two components of the electric field that are tangential to the air-substrate interface. Rather than decoupling them to obtain independent equations of the fourth order for each unknown, they are solved simultaneously by assuming that all fields have the same functional dependence along the y-direction (see Figs. 1 and 2). This procedure simplifies the derivation of the specific solutions to Maxwell's equations in the planar anisotropic region.

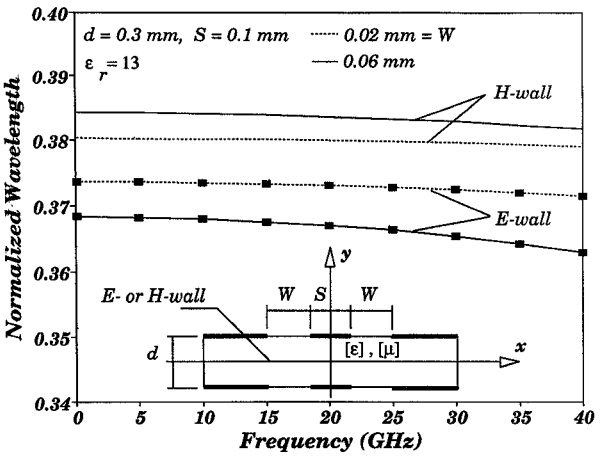

Fig. 1. Frequency dependence of ε_{eff} for open BCPWs: (_____ this method, ■■■ data from [2]).

Finally, a set of well-behaved basis functions are chosen to expand the fields across the two slots, and the Galerkin method is used to find a matrix system of linear equations, whose determinant contains the propagation constant. Specially, two kinds of symmetries (electric and magnetic walls) with respect to the $y = 0$ plane are considered, with numerical data provided for both. Very good agreement between the calculated results and those available in the literature is found for open as well as shielded structures.

II. The Spectral-Domain Formulation for BCPW's

The insets to Figs. 1 and 2 show the cross-sectional views of open and shielded BCPWs, along with their pertinent geometrical parameters d, S, and W. The metal strips are assumed to be perfectly conducting and infinitesimally thin. All structures possess two kinds of symmetries, that are defined according to whether the electric or magnetic wall is placed

Manuscript received September 20, 1992.

The authors are with the Department of Electrical and Computer Engineering, University of South Carolina, Columbia, SC 29208.

IEEE Log Number 9211845.

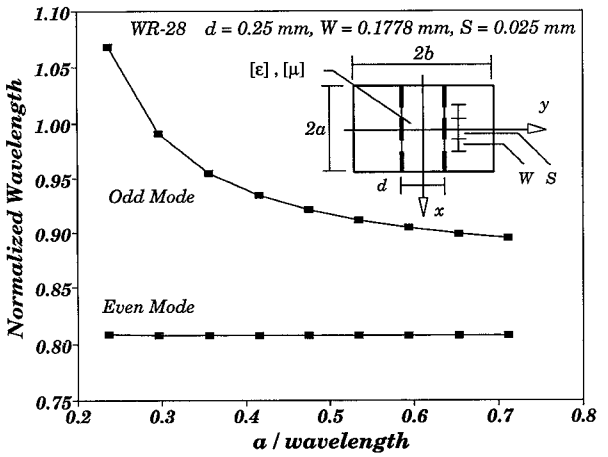

Fig. 2. Frequency dependence of ε_{eff} for a shielded BCPW ($2a = 7.112$ mm and $2b = 3.556$ mm): (_____ this method with $[\varepsilon_r] = \varepsilon_r[I], \varepsilon_r = 2.22$, and $[\mu_r] = [I]$; ■■■ data from [11]).

along the $y = 0$ plane. In order to avoid potential confusion in the terminology, the E- and M-wall nomenclature will refer to symmetries with respect to the y-direction, whereas the reference to the odd and even modes will correspond to symmetries in the x-direction. In this paper, an $e^{j(\omega t-\beta z)}$ time and z dependence is assumed for every field component, but is suppressed throughout. As usual, ω is the angular frequency and β is the unknown propagation constant, which is yet to be determined.

The theoretical formulation of the problem in the spectral-domain starts with the Fourier transformation of the vector wave equations for the fields with respect to the x-coordinate. As shown in [10], this procedure leads to the following set of independent matrix equations, one for $\tilde{\vec{E}}$ and $\tilde{\vec{H}}$, respectively:

$$\left[\tilde{\nabla}\times\right]\begin{Bmatrix}[\mu_r]^{-1}\\ [\varepsilon_r]^{-1}\end{Bmatrix}\left[\tilde{\nabla}\times\right]\begin{Bmatrix}|\tilde{E}\rangle\\ |\tilde{H}\rangle\end{Bmatrix} - k_0^2\begin{Bmatrix}[\varepsilon_r]\\ [\mu_r]\end{Bmatrix}\begin{Bmatrix}|\tilde{E}\rangle\\ |\tilde{H}\rangle\end{Bmatrix} = |0\rangle\,, \tag{1a,b}$$

where $|\tilde{E}\rangle$ and $|\tilde{H}\rangle$ are column vectors containing Cartesian components of $\tilde{\vec{E}}$ and $\tilde{\vec{H}}$, and $[\tilde{\nabla}\times]$ is the matrix differential operator defined in [10], with the permittivity and permeability tensors of the substrate given by

$$\left[\begin{pmatrix}\varepsilon_r\\ \mu_r\end{pmatrix}\right] = \begin{bmatrix}\begin{pmatrix}\varepsilon_{xx}\\ \mu_{xx}\end{pmatrix} & 0 & \begin{pmatrix}\varepsilon_{xz}\\ \mu_{xz}\end{pmatrix}\\ 0 & \begin{pmatrix}\varepsilon_{yy}\\ \mu_{yy}\end{pmatrix} & 0\\ \begin{pmatrix}\varepsilon_{zx}\\ \mu_{zx}\end{pmatrix} & 0 & \begin{pmatrix}\varepsilon_{zz}\\ \mu_{zz}\end{pmatrix}\end{bmatrix}. \tag{2a,b}$$

In this paper, the off-diagonal elements of the permittivity tensor represent the possible misalignment between the principal axes of the substrate (x_1, y_1, z_1) (where $[\varepsilon_r]$ is diagonal with elements $(\varepsilon_{x1}, \varepsilon_{y1}, \varepsilon_{z1})$) and the coordinates of the guide (x, y, z). At the same time, the substrate permeability tensor is assumed to become gyrotropic when exposed to an applied dc magnetic field. All tensor elements corresponding to the above material properties can be written as

$$\varepsilon_{xx} = \varepsilon_{x1}\cos^2\theta + \varepsilon_{z1}\sin^2\theta \qquad \varepsilon_{yy} = \varepsilon_{y1} \tag{3a,b}$$

$$\varepsilon_{zz} = \varepsilon_{x1}\sin^2\theta + \varepsilon_{z1}\cos^2\theta$$
$$\varepsilon_{xz} = \varepsilon_{zx} = (\varepsilon_{z1} - \varepsilon_{x1})\sin\theta\cos\theta \tag{3c,d}$$

$$\mu_{xx} = \mu_{zz} = \mu_d = 1 + \frac{\omega_0\omega_m}{\omega_0^2 - \omega^2}\,,$$
$$\mu_{yy} = 1\,, \qquad \mu_{xz} = -\mu_{zx} = jk_d = \frac{j\omega_m\omega}{\omega_0^2 - \omega^2}\,, \tag{4a,b,c}$$

where θ is the angle between coordinate axes (x, x_1) or (z, z_1). The permeability parameters of equation (4) are $\omega_0 = \mu_0\gamma_0 H_0, \omega_m = \mu_0\gamma_0 M_s$, with γ_0, H_0 and M_s being the gyromagnetic ratio, applied dc magnetic field, and magnetization of the ferrite, respectively.

The field representation in the anisotropic region can be obtained by solving (1a). Due to anisotropy, all components of the electric field are coupled, and the conventional procedure involves elimination of the component of $\tilde{\vec{E}}$ that is perpendicular to the interface $(\tilde{E}_y)$. After lengthy simplifications, the final set of fourth order independent differential equations for the tangential components of the electric field ($\tilde{E}_x$ and $\tilde{E}_z$) is usually obtained.

Instead, however, it is easier to solve two coupled second order equations for $\tilde{E}_x$ and $\tilde{E}_z$ directly. These components of electric field satisfy the following coupled set of equations:

$$\begin{bmatrix}\alpha_{11}^A\frac{d^2}{dy^2} + \alpha_{11}^B & \alpha_{12}^A\frac{d^2}{dy^2} + \alpha_{12}^B\\ \alpha_{21}^A\frac{d^2}{dy^2} + \alpha_{21}^B & \alpha_{22}^A\frac{d^2}{dy^2} + \alpha_{22}^B\end{bmatrix}\begin{bmatrix}\tilde{E}_x\\ \tilde{E}_z\end{bmatrix} = \begin{bmatrix}0\\ 0\end{bmatrix}, \tag{5}$$

where, α_{11}^A through α_{22}^B are given in the Appendix. The solution for both $\tilde{E}_x$ and $\tilde{E}_z$ is expected to have the same functional dependence along the y-direction, which in its most general form is $e^{\gamma y}$, except for multiplicative constant factors. Therefore, the characteristic equation for the transverse propagation constant, γ, is found by replacing d^2/dy^2 with γ^2 and setting the determinant of (5) equal to zero. Since the resulting characteristic equation for γ is a fourth order polynomial (see [10] for explicit form), having even order powers only, the solution can be expressed in terms of hyperbolic sine and cosine functions. The final expressions for $\tilde{E}_x$ and $\tilde{E}_z$ are then determined by enforcing the boundary conditions at the wall of symmetry, i.e., at $y = 0$. The remaining components of EM fields can now be obtained from Maxwell's equations directly.

The fields in the isotropic region can be found by using scalar electric and magnetic potentials [9, p. 337], which are a combination of the TE^y and TM^y waves. Once the components of the fields tangential to the air-substrate interface are available in each individual region, the dyadic Green's function can be derived by matching them at the interface $(y = d/2)$. This leads to

$$\begin{bmatrix}\tilde{G}_{zz}(\alpha,\beta) & \tilde{G}_{zx}(\alpha,\beta)\\ \tilde{G}_{xz}(\alpha,\beta) & \tilde{G}_{xx}(\alpha,\beta)\end{bmatrix}\begin{bmatrix}\tilde{E}_z(\alpha, d/2)\\ \tilde{E}_x(\alpha, d/2)\end{bmatrix} = \begin{bmatrix}\tilde{J}_z(\alpha)\\ \tilde{J}_x(\alpha)\end{bmatrix}, \tag{6}$$

where elements of $[\tilde{G}(\alpha,\beta)]$ are listed in the Appendix. It should be added that for the shielded structure α is a discrete transform variable associated with the x-coordinate, whereas for open structures it is assumed to be continuous extending from minus to plus infinity.

Finally, the Galerkin method is used to set up the eigenvalue problem for the propagation constant β. The fields inside the slots are expanded in terms of known basis functions with built-in singular properties at the edges of the slot. Specifically, in the space-domain, $E_x(x)$ and $E_z(x)$ are taken to be

$$(E_x(x);E_z(x)) = \sum_{m;n=1}^{\infty} (a_m E_{xm}(x); b_n E_{zn}(x)) \qquad (7a,b)$$

with

$$E_{xm}(x) = \frac{\cos\left[\frac{(m-1)\pi(x+B)}{(W/2)}\right]}{\sqrt{[W/2]^2-[(x+B)]^2}}\left[U\left(x+W+\frac{S}{2}\right) - U\left(x+\frac{S}{2}\right)\right] \mp \frac{\cos\left[\frac{(m-1)\pi(x-B)}{(W/2)}\right]}{\sqrt{[W/2]^2-[(x-B)]^2}}\left[U\left(x-\frac{S}{2}\right) - U\left(x-\frac{S}{2}-W\right)\right] \quad m=1,2,3,\cdots, \qquad (8a)$$

$$E_{zn}(x) = \frac{\sin\left[\frac{\pi n(x+B)}{(W/2)}\right]}{\sqrt{[W/2]^2-[(x+B)]^2}}\left[U\left(x+W+\frac{S}{2}\right) - U\left(x+\frac{S}{2}\right)\right] \pm \frac{\sin\left[\frac{\pi n(x-B)}{(W/2)}\right]}{\sqrt{[W/2]^2-[(x-B)]^2}}\left[U\left(x-\frac{S}{2}\right) - U\left(x-\frac{S}{2}-W\right)\right] \quad n=1,2,3,\cdots, \qquad (8b)$$

where geometrical parameters W and $S(B = (S+W)/2)$ are defined in Figs. 1 and 2. In the above equation, the upper signs on the right side refer to even modes, whereas the lower sign corresponds to the odd mode. The Heaviside function, $U(x \pm x_0)$, is 1 for $(x \pm x_0) \geq 0$ or 0 otherwise.

III. Numerical Results

Prior to presenting the numerical results for BCPWs printed on anisotropic substrates, the theoretical formulation is validated against previously published data. Figs. 1 and 2 contain the validation curves for open and shielded structures, respectively. When the substrate material of an open MIC is isotropic, with $\varepsilon_{xx} = \varepsilon_{yy} = \varepsilon_{zz} = 13$ and $\mu_{xx} = \mu_{yy} = \mu_{zz} = 1$, the normalized wavelength (λ_g/λ) is computed and plotted for both the E- and H-wall symmetries. Comparison is made for the E-wall with data available in [2]. As can be seen from Fig. 1, a very good agreement is observed for two different slot dimensions. In addition, numerical results for the shielded bilateral CPW were also calculated by the present method and compared to those available in [11]. Once again, as shown in Fig. 2, a very good agreement between the two sets of data was obtained.

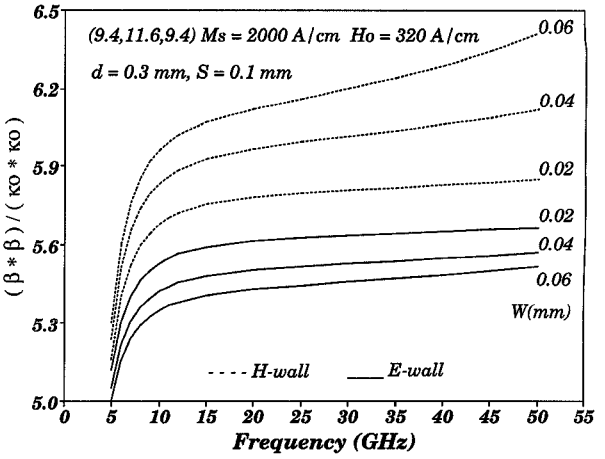

Fig. 3. $(n_{\text{eff}})^2$ as a function of the frequency for open BCPW without misalignment.

To see the influence that substrate anisotropy has on the propagation characteristics, namely on $n_{\text{eff}}^2 = (\beta/k_0)^2$, of open bilateral CPWs, different potential design parameters were varied, and the results are summarized in Figs. 3–5. In the remaining plots, the quantities inside parenthesis are the principal elements of $[\varepsilon]$, and γ_o is 1.759×10^{11} C/Kg. First, Fig. 3 shows the frequency response of an open MIC that is printed on anisotropic material, as a function of the changing slot width (W). It should be pointed out that the dispersion properties of the guided waves of E- and H-wall symmetries exhibit totally contrasting behavior. Most notable is the fact that n_{eff}^2 for the E-wall case decreases with increasing values of the slot width, while the opposite is true for the H-wall case.

Next, Figs. 4 and 5 illustrate what happens to n_{eff}^2 when the principal axes of the permittivity tensor are misaligned with those of the open BCPW waveguide. It can be seen from Fig. 4 that within the entire frequency range (with fixed waveguide dimensions), n_{eff}^2 of both the E- and H-wall symmetries decreases as the misalignment angle θ increases. Correspondingly, effects of changing θ on n_{eff}^2 at selected frequencies, when the CPW dimensions are held fixed, are shown in Fig. 5, which indicate an increase in n_{eff}^2 for larger values of the frequency.

The computed propagation characteristics for a shielded BCPW are displayed in Figs. 6 and 7. Numerical results for the dominant (H-wall) mode are plotted in Fig. 6 versus frequency for both odd and even modes. As can be seen, the even mode is far less dispersive compared to the odd mode of the shielded structure. It is also found that the effect of increasing slot width is to reduce n_{eff}^2 of both the odd and even modes.

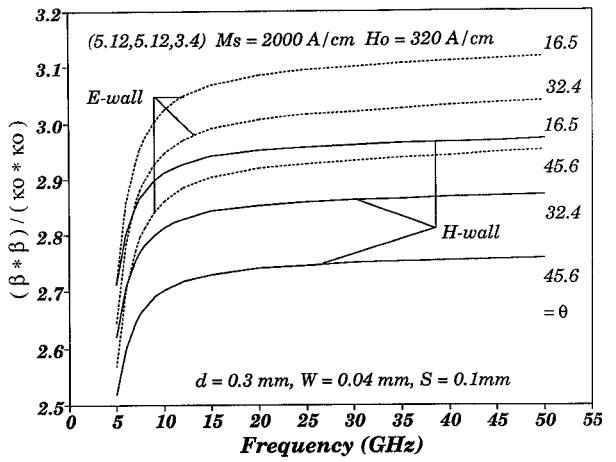

Fig. 4. $(n_{\text{eff}})^2$ as a function of the frequency for open BCPW with misalignment.

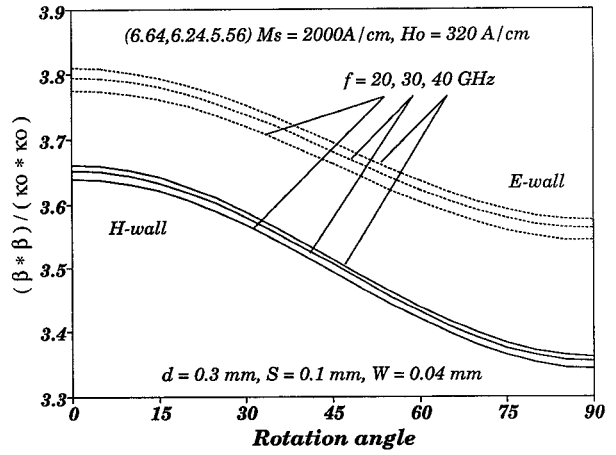

Fig. 5. $(n_{\text{eff}})^2$ of an open BCPW as a function of the rotation angle at $f =$ 20, 30, and 40 GHz.

Finally, in Fig. 7 the influence of the rotation angle θ on the propagation properties of shielded BCPW are shown for several frequencies (15, 30, and 50 GHz) when all physical dimensions of the waveguide are fixed. It is evident that the effects of misalignment on the shielded bilateral CPW are not as strong as on its open counterpart (see Fig. 5).

IV. Conclusion

In this paper, the spectral-domain method was used to study dispersion characteristics of open and shielded bilateral coplanar waveguides. The substrate material of every structure was assumed to be anisotropic in both $[\varepsilon]$ and $[\mu]$. The dyadic admittance Green's function was derived without resorting to fourth order independent differential equations, but rather by solving a coupled set of second order equations directly. A set of well behaved basis functions were used to expand the electric field within the CPW slots, and the Galerkin method was employed to find the propagation constant. Finally, numerous results examining effects on the propagation characteristics of the CPW with respect to frequency, slot width, and the misalignment angle of the permittivity tensor were presented.

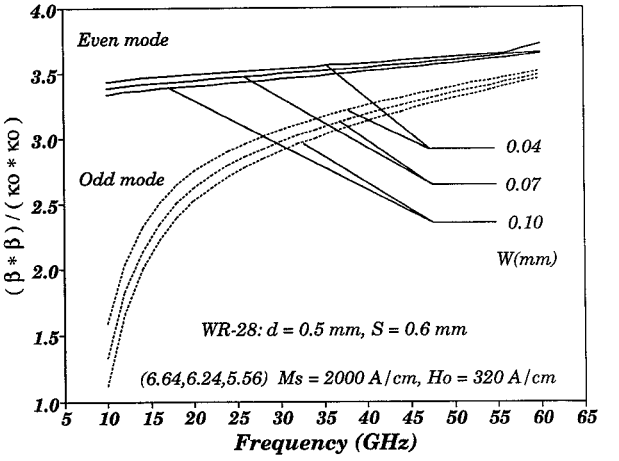

Fig. 6. $(n_{\text{eff}})^2$ as a function of the frequency for a shielded BCPW.

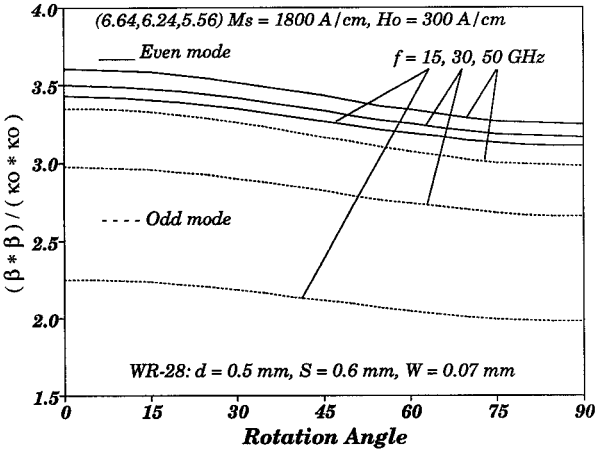

Fig. 7. $(n_{\text{eff}})^2$ for a shielded BCPW as a function of the rotation angle at $f = 15$, 30, and 50 GHz.

Appendix

The elements appearing in the matrix (5) are given by

$$\alpha^A_{(11;22)}\frac{d^2}{dy^2} + \alpha^B_{(11;22)} = \left(\beta^2\mu_d - k_0^2\varepsilon_{yy}\mu_{(xx;zz)}\mu_d\right)\frac{d^2}{dy^2} + \left(k_0^2\varepsilon_{(xx;zz)} - \frac{(\beta;\alpha)^2}{\mu_{yy}}\right)\mu_d G_0 \qquad \text{(A-1,2)}$$

$$\alpha^A_{(12;21)}\frac{d^2}{dy^2} + \alpha^B_{(12;21)} = \left(-\alpha\beta\mu_d - k_0^2\varepsilon_{yy}\mu_{(zx;xz)}\mu_d\right)\frac{d^2}{dy^2} + \left(k_0^2\varepsilon_{(xz;zx)} - \frac{\alpha\beta}{\mu_{yy}}\right)\mu_d G_0\,, \qquad \text{(A-3,4)}$$

where $\mu_d = \mu_{xx}\mu_{zz} - \mu_{xz}\mu_{zx}$, and

$$G_0 = \alpha^2\mu_{xx} + \alpha\beta(\mu_{xz} + \mu_{zx}) + \beta^2\mu_{zz} - k_0^2\varepsilon_{yy}\mu_d\,. \qquad \text{(A-5)}$$

In equations (A-1)–(A-5), β is the propagation constant, α is the Fourier transform variable, and k_0 is the propagation constant of the free space.

The elements of the dyadic admittance Green's function that was defined in equation (6) are written as

$$\tilde{G}_{zz}(\alpha,\beta) = \frac{1}{B_2 - B_1}(B_2 w_{11} - B_1 w_{12})$$
$$\tilde{G}_{zx}(\alpha,\beta) = \frac{1}{B_2 - B_1}(w_{11} - w_{12}) \qquad \text{(A-6a,b)}$$

$$\tilde{G}_{xz}(\alpha,\beta) = \frac{1}{B_2 - B_1}(B_1 w_{22} - B_2 w_{21})$$
$$\tilde{G}_{xx}(\alpha,\beta) = \frac{1}{B_2 - B_1}(w_{22} - w_{21}) \qquad \text{(A-6c,d)}$$

with $B_{1,2} = (\alpha_{12}^A \gamma_{a,b}^2 + \alpha_{12}^B)/(\alpha_{11}^A \gamma_{a,b}^2 + \alpha_{11}^B)$, and

$$w_{11,12} = \frac{\gamma_{a,b}}{z_t}(\alpha_{21}^A B_{1,2} - \alpha_{22}^A)\begin{pmatrix} th_{a,b}^m \\ ct_{a,b}^e \end{pmatrix} - \left\{ \frac{\beta(\beta - \alpha B_{1,2})}{\gamma_{y1}(\alpha^2+\beta^2)} + \frac{\alpha\gamma_{z1}(\alpha + \beta B_{1,2})}{(\alpha^2+\beta^2)} \right\}\begin{pmatrix} f^o \\ f^s \end{pmatrix} \qquad \text{(A-7a,b)}$$

$$w_{21,22} = \frac{\gamma_{a,b}}{z_t}(\alpha_{12}^A - \alpha_{11}^A B_{1,2})\begin{pmatrix} th_{a,b}^m \\ ct_{a,b}^e \end{pmatrix} + \left\{ \frac{\alpha(\beta - \alpha B_{1,2})}{\gamma_{y1}(\alpha^2+\beta^2)} - \frac{\beta\gamma_{z1}(\alpha + \beta B_{1,2})}{(\alpha^2+\beta^2)} \right\}\begin{pmatrix} f^o \\ f^s \end{pmatrix}, \qquad \text{(A-7c,d)}$$

where the Green's functions for different symmetries (E- or H-wall) of open or shielded structures are included in this compact form. The factors $th_{a,b}^m$ and $ct_{a,b}^e$ refer to the magnetic (H) and electric (E) wall, whereas $f^{o,s}$ corresponds to open or shielded BCPWs, with their explicit forms:

$$th_{a,b}^m = \tanh\left(\gamma_{a,b}\frac{d}{2}\right), \qquad ct_{a,b}^e = \coth\left(\gamma_{a,b}\frac{d}{2}\right), \qquad \text{(A-8a,b)}$$

$$f^o = 1, \qquad f^s = \coth\gamma_0\left(b - \frac{d}{2}\right). \qquad \text{(A-9a,b)}$$

The remaining parameters, appearing above, are defined as

$$\gamma_0 = \sqrt{\alpha^2 + \beta^2 - k_0^2}, \qquad z_t = j\omega\mu_0\mu_d G_0, \qquad \text{(A-10a,b)}$$

$$\gamma_{y1} = \gamma_0/(j\omega\varepsilon_0), \qquad \gamma_{z1} = \gamma_0/(j\omega\mu_0). \qquad \text{(A-11a,b)}$$

ACKNOWLEDGMENT

The authors wish to thank one anonymous reviewer for many helpful comments which improved the clarity of this paper.

REFERENCES

[1] R. W. Jackson, "Considerations in the use of coplanar waveguide for millimeter-wave integrated circuits," *IEEE Trans. Microwave Theory Tech.*, vol. MTT-34, no. 12, pp. 1450–1456, Dec. 1986.
[2] Y. C. Shinh and T. Itoh, "Analysis of conductor-backed coplanar waveguide," in *Microwave Integrated Circuits*, J. Frey Ed., 1982, pp. 62–63.
[3] T. Itoh, "Overview of quasi-plannar transmission lines," *IEEE Trans. Microwave Theory Tech.*, vol. 37, no. 2, pp. 275–280, Feb. 1989.
[4] C. P. Wen, "Coplanar waveguide: a surface strip transmission line suitable for nonreciprocal gyromagnetic device application," *IEEE Trans. Microwave Theory Tech.*, vol. MTT-17, no. 12, pp. 1087–1090, Dec. 1969.
[5] J. B. Knorr and K. D. Kuchler, "Analysis of coupled slots and coplanar strip on dielectric substrate," *IEEE Trans. Microwave Theory Tech.*, vol. MTT-23, no. 7, pp. 541–548, July 1975.
[6] T. Kitazawa and Y. Hayashi, "Coupled slots on an anisotropic substrate," *IEEE Trans. Microwave Theory Tech.*, vol. MTT-29, no. 10, pp. 1035–1040, Oct. 1981.
[7] E-B. El-Sharawy and R. W. Jackson, "Coplanar waveguide and slot line on magnetic substrates: Analysis and experiment," *IEEE Trans. Microwave Theory Tech.*, vol. 36, no. 6, pp. 1071–1079, June 1988.
[8] T. Kitazawa and T. Itoh, "Asymmetrical coplanar waveguide with finite metallization thickness containing anisotropic media," *IEEE Trans. Microwave Theory Tech.*, vol. 39, no. 8, pp. 1427–1433, Aug. 1991.
[9] T. Itoh, Ed., *Numerical Techniques for Microwave and Millimeter-wave Passive Structures.* New York: Wiley, 1989.
[10] Y. Chen and B. Beker, "Dispersion characteristics of open and shielded microstrip lines under a combined principal axes rotation of electrically and magnetically anisotropic substrates," *IEEE Trans. Microwave Theory Tech.*, vol. 41, no. 4, pp. 673–679, Apr. 1993.
[11] A. K. Sharma and W. J. R. Hoefer, "Propagation in coupled unilateral and bilateral finlines," *IEEE Trans. Microwave Theory Tech.*, vol. MTT-31, no. 6, pp. 498–502, June 1983.
[12] M. Tsuji, H. Shigesawa, and A. A. Oliner, "New interesting leakage behavior on coplanar waveguides of finite and infinite widths," *IEEE Trans. Microwave Theory Tech.*, vol. 39, no. 12, pp. 2130–2137, Dec. 1991.

Yinchao Chen, photograph and biography not available at the time of publication.

Benjamin Beker photograph and biography not available at the time of publication.